

# Mitochondria permeability transition-dependent *tert*-butyl hydroperoxide-induced apoptosis in hepatoma HepG2 cells

Jean-Pascal Piret<sup>a,\*</sup>, Thierry Arnould<sup>a</sup>, Bruno Fuks<sup>b</sup>, Pierre Chatelain<sup>b</sup>,  
José Remacle<sup>a</sup>, Carine Michiels<sup>a</sup>

<sup>a</sup>Laboratory of Biochemistry and Cellular Biology, Facultés Universitaires Notre-Dame de la Paix,  
61 rue de Bruxelles, 5000 Namur, Belgium

<sup>b</sup>In Vitro Pharmacology Department, UCB Pharma, Chemin du Foriest,  
1420 Braine-l'Alleud, Belgium

Received 25 February 2003; accepted 15 September 2003

## Abstract

*Tert*-butyl hydroperoxide (*t*-BHP) has been demonstrated to induce apoptosis in hepatoma cell line HepG2, but poor data were available on the signaling pathway initiated by *t*-BHP. In this work, we studied in details the apoptotic pathways induced in HepG2 cells by *t*-BHP. DNA fragmentation, activation of caspases and cytochrome *c* release were demonstrated. Permeability transition pore inhibitors prevented the DNA fragmentation and caspase activation induced by *t*-BHP. In addition, changes in the mitochondrial membrane potential were detected: hyperpolarization preceded loss of membrane potential. It also preceded caspase activation which occurred before the induction of DNA fragmentation. Taken together, these results emphasize the central role played by mitochondria in the initiation of apoptosis in HepG2 cells exposed to oxidant agents.

© 2003 Elsevier Inc. All rights reserved.

**Keywords:** Mitochondria; DNA fragmentation; Caspase; Permeability transition pore

## 1. Introduction

Apoptosis is a normal biological process by which pluricellular organisms maintain homeostasis of their tissues [1]. During development, apoptosis helps to sculpture the body, shape the organs and carve out the fingers and toes [2]. This process is also important for the regulation of the immune system and for the elimination of pathogen-infected cells [3]. However, apoptosis has to be tightly regulated as too little or too much cell death may lead to pathology, including developmental defects, autoimmune diseases, neurodegeneration or cancer. Apoptosis results in a reduction in cell volume, membrane blebbing and chromatin condensation, reducing the cells to shrivelled corpses that are rapidly taken

up by phagocytes or neighboring cells. Apoptosis can be differentiated from other forms of cell death, termed necrosis or “accidental” cell death which is characterized by swelling of cells and disruption of membranes causing inflammation of neighboring tissues. Apoptosis can be induced by different external or internal stimuli like withdrawal of growth factors, presence of cytokine (TNF- $\alpha$ , Fas ligand), DNA damages, viruses, oxidative stresses, etc.

*t*-BHP has been reported to induce apoptosis in the brain *in vivo* [1] and in hepatocytes *in vitro* [4]. Lipidic hydroperoxides are formed in living cells by lipid peroxidation via formation of oxygen-derived free radicals from multiple sources like oxidative stresses, enzymatic reactions or xenobiotics. *t*-BHP is a short chain analog of lipid hydroperoxides which mimics the toxic effect of peroxidized fatty acids. Peroxy radicals can be generated from *t*-BHP in the cytosol by its interaction with ferrous iron in a reaction similar to the Fenton reaction [5]. It has also been reported that *t*-BHP leads to cell death by inducing changes in mitochondrial permeability in hepatocytes accompanied by a depolarization of the mitochondrial potential [6,7].

\* Corresponding author. Tel.: +32-81-724129; fax: +32-81-724135.

E-mail address: [jppiret@fundp.ac.be](mailto:jppiret@fundp.ac.be) (J.-P. Piret).

Abbreviations: BA, bongkreikic acid; CyA, cyclosporin A; FCCP, carbonylcyanide-*p*-trifluoromethoxyphenyl hydrazone; LDH, lactate dehydrogenase; MPTP, mitochondrial permeability transition pore; ROS, reactive oxygen species; *t*-BHP, *tert*-butyl hydroperoxide; TFP, trifluoperazine; TMRE, tetramethylrhodamine ethyl ester.

The MPTP is a high-conductance unselective channel composed by the apposition of proteins from the inner and outer mitochondrial membrane at contact sites between the two membranes [8,9]. The MPTP is probably formed by the association of adenine nucleotide translocator, voltage-dependent anion channel and cyclophilin D. Other proteins have been proposed to be part of the pore: creatine kinase, hexokinase and the peripheral benzodiazepine receptor [10,11]. MPTP opening causes a sudden increase in the permeability of the inner mitochondrial membrane to molecules of mass <1.5 kDa. This event, called “mitochondrial permeability transition”, results in the dissipation of the mitochondrial potential, uncoupling of oxidative phosphorylation and chemical equilibration between cytoplasm and mitochondrial matrix [9,12]. Depending on the extent of pore opening, this process causes a progressive osmotic swelling of the mitochondrial matrix and finally a transient or long lasting disruption of the outer membrane. However, the role of MPTP opening in inducing cytochrome *c* release remains unclear.

In the present study, we studied in details the apoptotic signaling pathway induced by *t*-BHP in human hepatoma cell line HepG2. Cytochrome *c* release, caspase activation and DNA fragmentation were observed and their kinetics studied. Moreover, we demonstrated that *t*-BHP seems to activate the execution phase of apoptosis at least in part through the MPTP.

## 2. Materials and methods

### 2.1. Cell culture

Human hepatoma cells HepG2 were maintained in culture in 75-cm<sup>2</sup> polystyrene flasks (Costar) with 15 mL of Dulbecco's modified Eagle's medium (DMEM) liquid (with sodium pyruvate; 1000 mg/L; pyridoxine) containing 5 mL/500 mL of Pen-Strep (Biowhittaker Europe) and 10% of fetal calf serum and incubated under an atmosphere of 5% CO<sub>2</sub>.

### 2.2. *t*-BHP incubation

All experiments for assaying DNA fragmentation or LDH release were performed 1 day after plating 50,000 cells in 500 µL of the above medium into 1.88 cm<sup>2</sup> wells of a 24-well microtiter plate (Costar).

Cells were pretreated for 30 min in medium without serum containing one of the following chemicals. Cyclosporin A (Sigma) was dissolved in ethanol; trifluoperazin (Sigma) and bongkreikic acid (Calbiochem) in deionized filtrated water. After 30 min of pretreatment, these different chemicals were added in DMEM without serum containing *t*-BHP (Merck; final concentration:  $5 \times 10^{-4}$  M) for different incubation times. Solvent concentration was always below 0.2%.

The pan caspase inhibitor zVAD-fmk (R&D Systems, dissolved in DMSO) was added directly, without pretreatment, in DMEM without serum containing *t*-BHP ( $5 \times 10^{-4}$  M).

### 2.3. Viability

In order to estimate cell viability, directly after the incubations, the medium was removed and cells were stained with a solution containing 10 µg/mL ethidium bromide and 3 µg/mL acridine orange in PBS. Viable cells appear green while cells with permeabilized plasma membrane are orange when observed in fluorescence microscopy.

### 2.4. DNA fragmentation and LDH release

The measurement of cytoplasmic histone-associated DNA fragments (mono- and oligonucleosomes) after induction of cell death was performed with the “cell death detection ELISA” (Roche Molecular Biochemicals). After the incubation, cells were lysed with the incubation buffer as described by the manufacturer and the cytoplasmic fraction recovered.

ELISA was also performed according to the manufacturer's protocol. For the determination of *t*-BHP cytotoxicity, LDH release was measured with the “cytotoxicity detection kit” from Roche Molecular Biochemical according to the manufacturer's protocol. The culture media from incubated cells were removed and centrifuged to pellet the cell fragments and apoptotic bodies. In order to lyse the cells, Triton X-100 (Merck) at 10% in DMEM was added on this pellet as well as on the cells remaining in the wells. The percentage LDH release was calculated as follows:

LDH activity in medium (1) + LDH activity of cell fragments (2)/(1) + (2) + LDH activity of cells remaining in the wells.

### 2.5. DNA extraction and migration on agarose gel

After *t*-BHP ( $5 \times 10^{-4}$  M) incubation, cells from 75-cm<sup>2</sup> polystyrene flasks (Costar) were scrapped in 1 mL of lysis buffer (100 mM NaCl, 10 mM Tris, 25 mM EDTA, 0.5% SDS, pH 8) containing proteinase K (0.4 mg/mL) and incubated overnight at 37°. One volume of chloroform/phenol/isoamylalcohol was added to each sample before vortexing several seconds. The aqueous phase was recovered and 1 vol. of chloroform was added before vortexing several seconds. 0.7 vol. of isopropanol was added to the aqueous phase, vortexed and put at –20° overnight. The next day, samples were centrifuged for 30 s at 13,000 rpm at 4°. The supernatant was removed and 1 mL 70% ethanol was added at room temperature before a centrifugation at 13,000 rpm for 2 min. The pellet was then dried 3 min with a speedvac (Hetovac VR-1, Heto) and was resuspended in 100 µL of Tris-EDTA, pH 8 + RNase A (final concentration: 0.2 mg/mL) 2 hr at 37°. DNA was loaded on a 1.5%

agarose gel and migrated 2 hr at 90 V. The DNA ladder is the 100 bp DNA ladder (Promega).

## 2.6. Caspase activity assay

Fifty thousand cells were plated into a 24-well microtiter plate (Costar). One day later, cells were incubated in the presence of *t*-BHP ( $5 \times 10^{-4}$  M) for different incubation times. Caspase activity was assayed using the fluorimetric “homogeneous caspase assay” kit from Roche Molecular Biochemicals. After the incubation, the culture medium was removed and 100  $\mu$ L of the incubation solution containing a fluorescent substrate (DEVD-Rhodamine 110) were added into each well and incubated 2 hr at 37°. The fluorescence was measured with a microplate fluorescence reader (FLUO star) at an excitation wavelength of 515 nm and an emission wavelength of 555 nm.

Active caspase 3 was quantitated using an ELISA (Quantikine human active caspase 3 from R&D Systems) according to the manufacturer protocol.

## 2.7. Immunofluorescence

Cells were seeded on glass cover slides 1 day before the incubation. After the incubation, cells were fixed 10 min with 4% paraformaldehyde in PBS before to be washed  $3 \times 5$  min in PBS. Cells were permeabilized in PBS + 1% Triton X-100 and then washed  $3 \times 10$  min in PBS + 3% BSA (Sigma). The primary antibody (anti-active caspase 9 from Cell Signaling, 1:100 dilution) was added in PBS + 3% BSA overnight at 4° in wet room. The next day, cells were washed  $3 \times 10$  min in PBS + 3% BSA before the secondary antibody (Alexa Fluor 488 goat anti-mouse IgG (H + L) conjugate (Molecular Probes) were used at 1:500 dilution) was added in PBS + 3% BSA for 1 hr. Cells were washed  $3 \times 10$  min in PBS + 3% BSA. For nucleus labeling, the cells were incubated with TO-PRO-3 (dil 1/80, Molecular Probes). The cover slips were finally mounted in mowiol (Aldrich) and observed with a confocal microscope TCS (Leica).

## 2.8. Protein extracts and cytochrome *c* western blotting analysis

After *t*-BHP ( $5 \times 10^{-4}$  M) incubation, cells from 75-cm<sup>2</sup> polystyrene flasks (Costar) were trypsinized (with trypsin + EDTA for HepG2 cells). Cells were resuspended in cold PBS and centrifuged for 5 min at 1000 rpm. Cells were resuspended in 300  $\mu$ L of lysis buffer (220 mM mannitol, 68 mM sucrose, 50 mM KCl, 50 mM PIPES–KOH, 5 mM EGTA, 2 mM MgCl<sub>2</sub>, 1 mM DTT), and a protease inhibitor mixture (“Complete” from Roche Molecular Biochemicals, added at a 1:25 dilution). Cells were lysed with a Dounce glass homogenizer (10 or 15 passages) and centrifuged for 15 min at 13,000 rpm at 4°. The supernatant corresponds to a soluble fraction. Proteins

were then separated by SDS–PAGE on 15% acrylamide gel and transferred to a polyvinylidene difluoride membrane (Bio-Rad). The membrane was blocked with TBS–Tween 5% fat milk (Gloria) for 1 hr, followed by an incubation for 2 hr with the primary antibody in TBS–Tween 0.1% milk. After three times washes in TBS–Tween 0.1% 5 min, the incubation with the secondary antibody was performed for 30 min in TBS–Tween 0.1% milk followed by three washes for about 15 min in TBS–Tween. Finally, the membrane was revealed by enhanced chemiluminescence (New Life Science Products). Mouse anti-cytochrome *c* monoclonal antibody (Pharmingen) was used at 1:250 dilution and sheep anti-mouse IgG horseradish peroxidase-linked antibody (Amersham Pharmacia Biotech) was used at 1:2000 dilution as secondary antibody.

## 2.9. Protein extracts, Bcl-2 western blot analysis and cytochrome *c* ELISA

After *t*-BHP ( $5 \times 10^{-4}$  M) incubation, cells from 75-cm<sup>2</sup> polystyrene flasks (Costar) were scraped in 300  $\mu$ L of cold imidazol buffer (imidazol 3 mM, sucrose 250 mM, pH 7.4) and lysed with a Dounce glass homogenizer (20 passages). They were then centrifuged for 10 min at 1500 rpm to pellet unbroken cells and nuclei. The supernatant was centrifuged for 2 min at 13,000 rpm and the pellet was used as the mitochondrial fraction. The supernatant was centrifuged for 1 hr at 4° at 39,000 rpm and the supernatant corresponds to cytosolic extract. Proteins were then separated by SDS–PAGE on 15% acrylamide gel and transferred to a nitrocellulose membrane (Bio-Rad). The membrane was treated as recommended by Upstate. Finally, the membrane was revealed by enhanced chemiluminescence (New Life Science Products). Mouse anti-Bcl-2 monoclonal antibody (Upstate) was used at 1:1000 dilution and sheep anti-mouse IgG horseradish peroxidase-linked antibody (Amersham Pharmacia Biotech) was used at 1:10,000 dilution as secondary antibody. The membrane was rehybridized with anti-cytochrome oxidase subunit I antibody (Molecular Probes, 1:1000 dilution) to assay for the amount of mitochondrial proteins loaded on the gel. Cytochrome *c* in the cytosolic fractions was quantitated using an ELISA (Quantikine human cytochrome *c* from R&D Systems) according to the manufacturer protocol.

## 2.10. Mitochondrial membrane potential measurement

Mitochondrial membrane potential was studied by following the fluorescence of TMRE probe (Molecular Probes). HepG2 cells were cultivated on glass cover slide 2 days before the incubation. Cells were incubated with or without *t*-BHP ( $5 \times 10^{-4}$  M) in DMEM without serum for increasing times and the TMRE probe (1  $\mu$ M) was added during the last hour of incubation. The fluorescence associated with TMRE was followed with a fluorometer (Kontron instruments) with an excitation wavelength of

523 nm and an emission wavelength of 610 nm. After 1 and 6 hr, 10  $\mu$ M of the uncoupler FCCP (Sigma) was added during 15 min.

Rhodamine 123 probe (1  $\mu$ M) was added during the last 30 min of incubation. After 1 hr, 10  $\mu$ M of the FCCP was

added during 35 min. The supernatant was discarded and cells were washed 2 times with HBBS + CaCl<sub>2</sub>, pH 7.4. Then, cells were lysed by addition of passive lysis buffer (Promega) and shaken 10 min before being centrifuged for 2 min at 13,000 rpm. One hundred microliters of

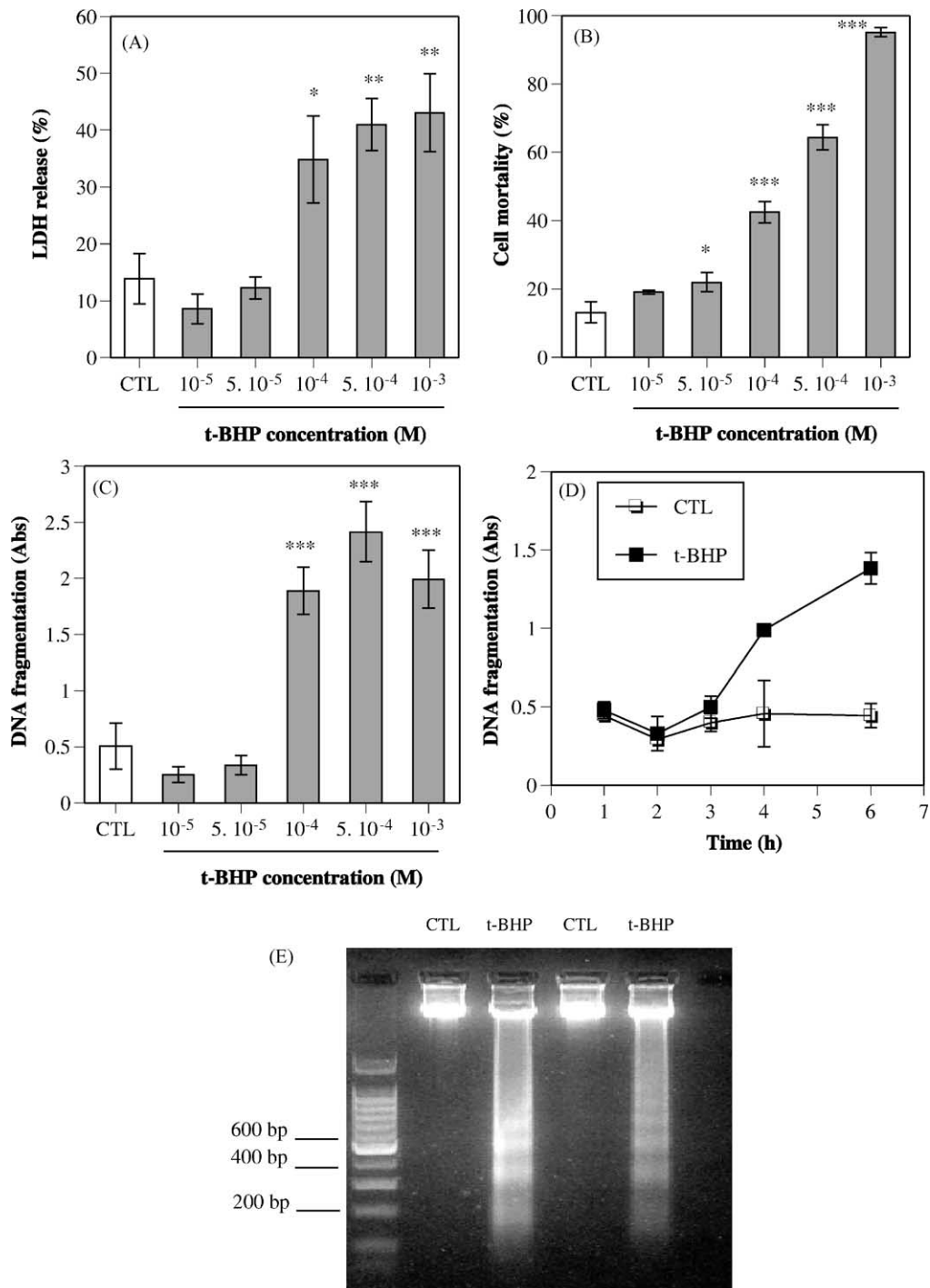


Fig. 1. *t*-BHP-induced LDH release and DNA fragmentation. Human HepG2 hepatoma cells were incubated with 0–10<sup>-3</sup> M *t*-BHP for 6 hr. (A) The release of LDH was assayed. (B) Viable cells were counted after staining with ethidium bromide/acridine orange. (C) DNA fragmentation was assayed using an ELISA for soluble nucleosomes. Results are expressed as means  $\pm$  1 SD (N = 3). \**P* < 0.05, \*\**P* < 0.01 and \*\*\**P* < 0.001 vs. control. (D) DNA fragmentation was assayed using an ELISA for soluble nucleosomes after different incubation times. Results are expressed as means  $\pm$  1 SD (N = 3). (E) HepG2 cells were incubated in the absence (CTL) or in the presence of 5  $\times$  10<sup>-4</sup> M *t*-BHP for 6 hr. DNA was extracted and electrophoresed on a 1.5% agarose gel. Lane 1: 100 base pair standard ladder (Promega). Results from two experiments.

supernatant were collected and the fluorescence associated to the Rhodamine 123 probe was measured using a fluorometer (Fluostar, BMG Labtechnologies) with an excitation wavelength of 485 nm and an emission wavelength of 520 nm.

### 2.11. Statistical analysis

Values are expressed as means  $\pm$  SD. Data were analyzed by ANOVA followed by Scheffe's contrasts.

## 3. Results

### 3.1. Induction of apoptosis by *t*-BHP in HepG2 cells

In order to study whether *t*-BHP was able to induce toxicity in HepG2 cells, the cytotoxicity of *t*-BHP was

investigated by measurement of LDH release and staining with ethidium bromide/acridine orange. Increasing concentrations of *t*-BHP induced a dose-dependent increase in toxicity as shown by the increase in the release of LDH (Fig. 1A). A parallel concentration curve was observed using ethidium bromide/acridine orange staining (Fig. 1B). This cytotoxic effect is, at least in part, due to apoptosis since a concentration-dependent increase in DNA fragmentation was also observed (Fig. 1C). These results indicate that *t*-BHP induced probably both necrosis and apoptosis. The increase in LDH release could also be the result of secondary necrosis that occurs after apoptosis in cultured cells. Concentration of  $5 \times 10^{-4}$  M of *t*-BHP was chosen for the following experiments. The time course of *t*-BHP-induced DNA fragmentation was followed: DNA fragmentation was detected after 4 hr incubation and increased further at 6 hr (Fig. 1D). In addition, 6 hr incubation in the presence of *t*-BHP induced a typical "DNA ladder"

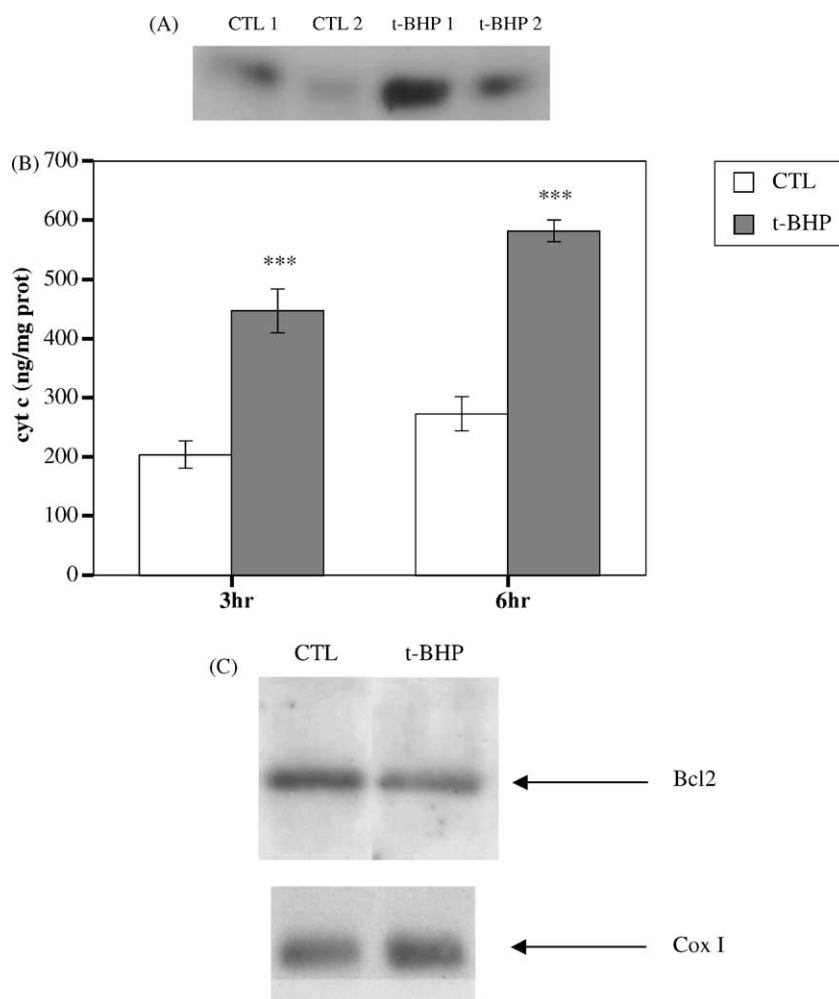


Fig. 2. *t*-BHP-induced cytochrome *c* release and decrease in Bcl-2 level. (A) HepG2 cells were incubated with (*t*-BHP 1 and *t*-BHP 2) or without (CTL 1 and CTL 2) *t*-BHP ( $5 \times 10^{-4}$  M) during 6 hr. Cells from the samples CTL 1 and *t*-BHP 1 were lysed by 15 passages in Dounce and CTL 2 and *t*-BHP 2 were lysed by 10 passages in Dounce. Soluble fractions were analyzed by western blot with a mouse anti-cytochrome *c* antibody. (B) HepG2 cells were incubated with or without *t*-BHP ( $5 \times 10^{-4}$  M) during 3 and 6 hr. Pure cytosolic fractions were analyzed for cytochrome *c* by ELISA. Results are expressed in ng of cytochrome *c*/mg of proteins as means  $\pm$  1 SD (N = 3). \*\*\* $P$  < 0.001 vs. control. (C) HepG2 cells were incubated with or without *t*-BHP ( $5 \times 10^{-4}$  M) during 3 hr. Pure mitochondrial fractions were analyzed for Bcl-2 and the subunit I of cytochrome oxidase by western blot.

pattern after migration of DNA on agarose gel (Fig. 1E). Moreover, this concentration of  $5 \times 10^{-4}$  M *t*-BHP-induced (already after 4 hr) typical nuclear morphology changes like chromatin condensation and nuclear fragmentation as revealed by Hoechst staining (data not shown).

We also studied Bcl-2-family proteins in different subcellular compartments following *t*-BHP incubation. First, Bax subcellular localization was investigated by immunofluorescence labeling and confocal microscopy. The results indicated that Bax was already present in the mitochondria of control cells and there was no change in location induced by *t*-BHP (data not shown). Second, following exposure of cells to apoptotic stimuli, cytochrome *c* can be rapidly released from mitochondria into the cytosol where, in combination with Apaf-1, it activates caspase 9 which in turn activates caspase 3, finally leading to the apoptotic cell death. The release of cytochrome *c* from mitochondria was detected in soluble fraction from *t*-BHP-incubated HepG2 (Fig. 2A). After 6 hr incubation, *t*-BHP-induced an increase in the release of cytochrome *c* of about 2.5-fold in comparison with controls. The amount of proteins loaded on the gel was similar for the different samples as estimated by coloration of the membrane with Coomassie blue (data not shown). The results were confirmed by assaying the

amount of cytochrome *c* present in a pure cytosolic fraction by ELISA: a 2-fold increase was observed after 3 hr incubation which was even higher after 6 hr (Fig. 2B). Third, cell fractionation was performed and Bcl-2 expression was investigated by western blot. Bcl-2 was detected in the mitochondrial fraction but not in the cytosolic one in control cells. After 3 hr incubation in the presence of *t*-BHP, Bcl-2 expression was decreased in the mitochondria without any detection of this protein in the cytosolic fraction (Fig. 2C).

Caspase activation is the initiating trigger of the apoptosis cascade and we verified that these enzymes were activated in HepG2 cells incubated in the presence of *t*-BHP. *t*-BHP-induced the activation of caspases, shown by the quantitation of active caspase 3, which started at 2 hr incubation and increased further afterwards (Fig. 3A). The *t*-BHP-induced caspase activation was totally inhibited by 0.1  $\mu$ M zVAD-fmk after 3 hr incubation (Fig. 3B).

The pan caspase inhibition zVAD-fmk was also able to inhibit the *t*-BHP-induced DNA fragmentation in a dose-dependent manner with a maximal inhibition between 10 and 1  $\mu$ M (Fig. 4C). In addition, two other caspase inhibitors have been tested on the *t*-BHP-induced DNA fragmentation: zLEHD-fmk which is more specific for caspase-9 and zIETD-fmk which is more specific for

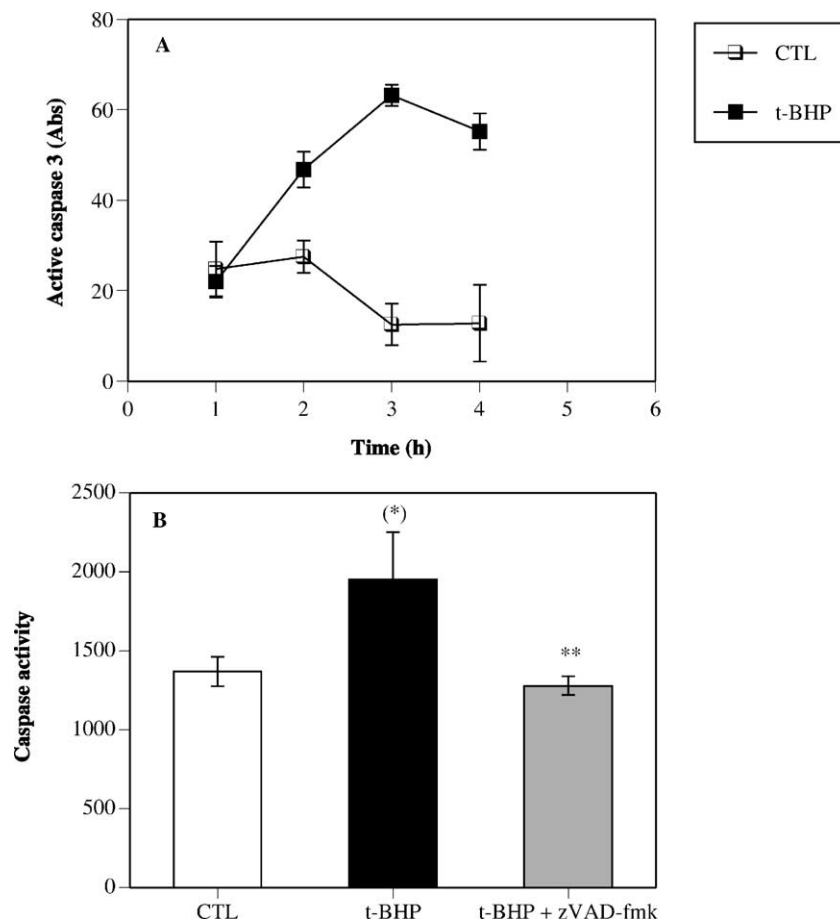


Fig. 3. Caspase activation. (A) HepG2 cells were incubated during increasing times with or without *t*-BHP ( $5 \times 10^{-4}$  M). Active caspase 3 was assayed as described in Section 2. (B) HepG2 cells were incubated 3 hr with *t*-BHP ( $5 \times 10^{-4}$  M) with or without zVAD-fmk (0.1  $\mu$ M). Caspase activity was assayed as described in Section 2. Results are expressed as means  $\pm$  1 SD (N = 3). (\*)  $P < 0.05$  vs. control; \*\*  $P < 0.01$  vs. *t*-BHP.



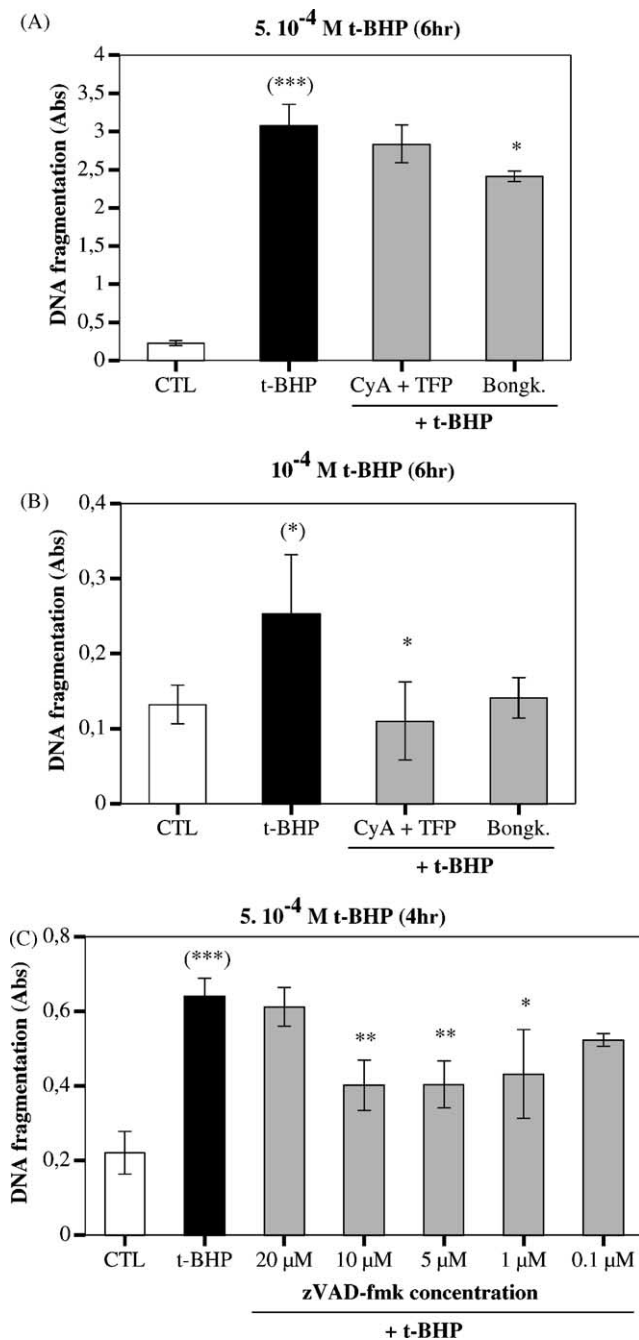


Fig. 4. Effect of cyclosporin A/TFP, bongkreic acid and zVAD-fmk on *t*-BHP-induced DNA fragmentation. (A, B) 50,000 cells/well were preincubated 30 min with different inhibitors then incubated in the presence of *t*-BHP: CyA (1 μM), TFP (5 μM) and bongkreic acid (Bongk., 100 μM). HepG2 cells were incubated for 6 hr with *t*-BHP (5 × 10<sup>-4</sup> M) (A) or 10<sup>-4</sup> M (B) in the presence or absence of inhibitors. DNA fragmentation was assayed by ELISA. Results are expressed as means ± 1 SD (N = 3). (\*) *P* < 0.05 vs. control; \*\* *P* < 0.05 vs. *t*-BHP; \*\*\* *P* < 0.001 vs. control. (C) HepG2 cells were incubated in the presence of *t*-BHP (5 × 10<sup>-4</sup> M) with or without different concentrations of zVAD-fmk for 4 hr. DNA fragmentation was assayed by ELISA. Results are expressed as means ± 1 SD (N = 3). (\*) *P* < 0.05 vs. *t*-BHP; \*\* *P* < 0.01 vs. *t*-BHP; \*\*\* *P* < 0.001 vs. control.

caspase-8. The results showed that the caspase-8 inhibitor did not inhibit *t*-BHP-induced DNA fragmentation. This result is consistent since this caspase is mainly activated through TNF-receptor or through Fas ligation. On the other

hand, caspase-9 inhibitor inhibited by 28% *t*-BHP-induced DNA fragmentation (data not shown).

The activation of caspase 9 was followed using an antibody specific of the active form of caspase 9. Cells were incubated 1.5 hr in the presence of *t*-BHP and then fixed, permeabilized and stained by immunofluorescence labeling. An increase in the level of active caspase 9 was evidenced in *t*-BHP-incubated cells in comparison to control cells. In addition, staining associated with the plasma membrane and into the nucleus was observed (Fig. 5B).

Taken together, these results indicate that *t*-BHP is able to induce cell death through apoptosis in HepG2 cells and that activation of caspase is involved.

### 3.2. Involvement of MPTP in HepG2 cells incubated with *t*-BHP

In order to investigate the possible involvement of MPTP in the apoptotic process triggered by *t*-BHP, the effect of two different MPTP inhibitors was tested on DNA fragmentation. As shown in Fig. 4B, CyA, a potent inhibitor of the MPTP in liver mitochondria [13] partially inhibited the *t*-BHP-induced DNA fragmentation in HepG2 cells in the presence of TFP (a non-specific phospholipase A2 inhibitor) when 10<sup>-4</sup> M of *t*-BHP was used. Moreover, the more selective inhibitor of the PTP, BA [14] which binds to the mitochondrial adenine nucleotide translocator, decreased the *t*-BHP-induced DNA fragmentation in HepG2 cells by 23% when 5 × 10<sup>-4</sup> M *t*-BHP was used (Fig. 4A) and by 93% in the presence of 10<sup>-4</sup> M of *t*-BHP (Fig. 4B). A parallel inhibition of *t*-BHP-induced increase in LDH release was observed in the presence of CyA + TFP or BA but the extent of inhibition was lower than the one observed on DNA fragmentation (data not shown).

In order to confirm the involvement of MPTP in the initiation of the apoptosis process, the effect of BA was also tested on caspase activation. The results showed that BA inhibited the caspase 3 activation induced by *t*-BHP (Fig. 5A). In addition, BA also prevented the activation of caspase-9 demonstrated by using the antibody directed against the active form of this caspase (Fig. 5B).

These results indicate that opening of the MPTP could be part of the initiating process triggering caspase activation and DNA fragmentation.

Direct measurements of the mitochondrial membrane potential were then performed in order to follow the kinetics of MPTP opening. In three independent experiments using TMRE as a probe, an hyperpolarization was observed after 1 hr incubation in the presence of 5 × 10<sup>-4</sup> M *t*-BHP which was followed by a depolarization after 4 and 6 hr incubation (Fig. 6A). In order to avoid the possibility of an artifactual effect of this fluorescent probe, a second probe was used, rhodamine 123. As previously shown, an hyperpolarization was observed after 1 hr incubation in the presence of *t*-BHP which was followed by a depolarization (Fig. 6B).

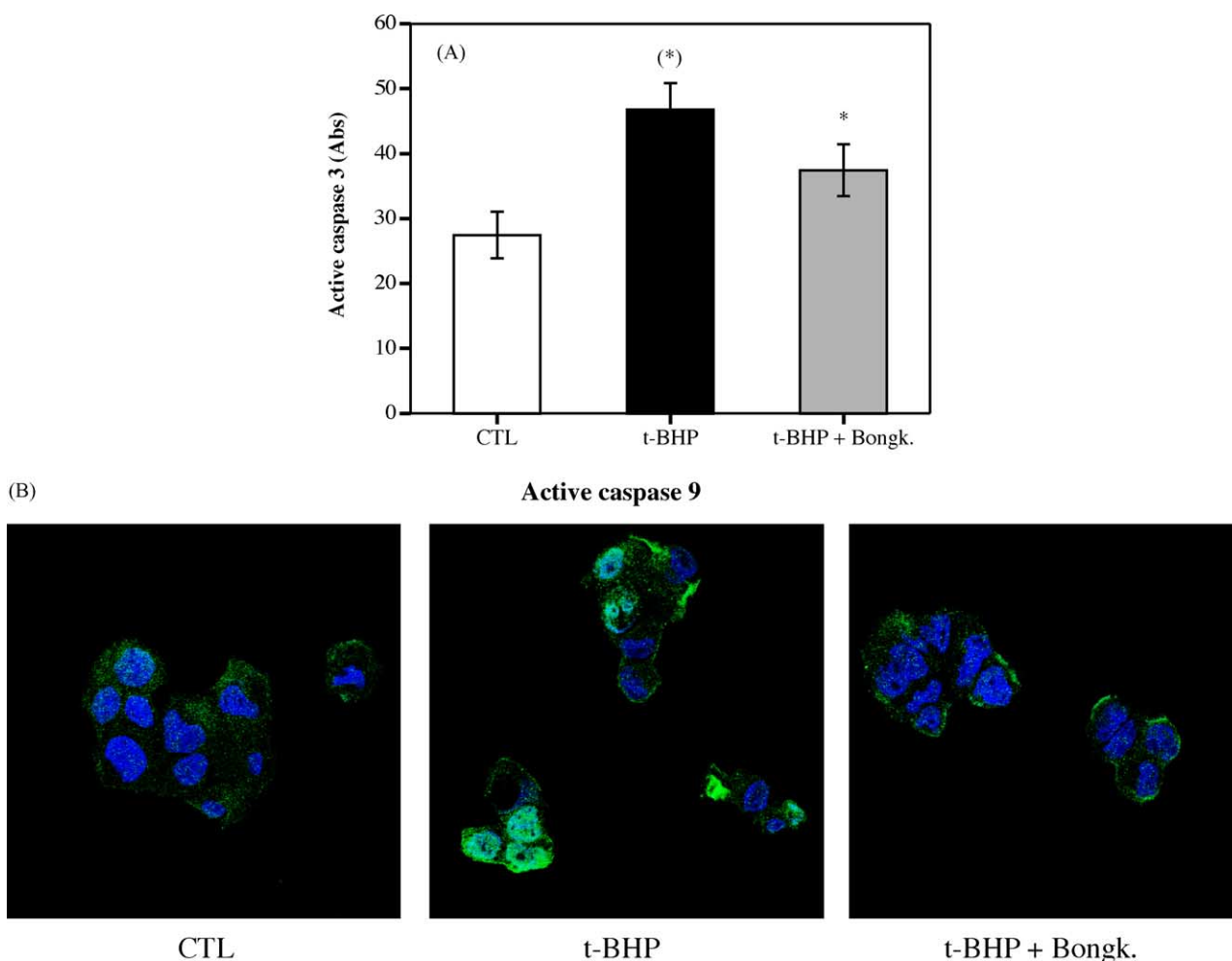


Fig. 5. Effect of bongkreikic acid on *t*-BHP-induced caspase activation. (A) HepG2 cells were incubated 2 hr with *t*-BHP ( $5 \times 10^{-4}$  M) with or without bongkreikic acid (Bongk., 100  $\mu$ M). Active caspase 3 was assayed as described in Section 2. Results are expressed as means  $\pm$  1 SD (N = 3). (\* $P$  < 0.05 vs. control; \* $P$  < 0.05 vs. *t*-BHP. (B) HepG2 cells were incubated 1.5 hr with *t*-BHP ( $5 \times 10^{-4}$  M) with or without bongkreikic acid (100  $\mu$ M). Active caspase 9 was detected by immunofluorescence labeling (green). Nuclei were stained with TO-PRO-3 (blue). Cells were observed in semi-quantitative confocal microscopy.

#### 4. Discussion

In the present study, the apoptotic pathway induced by *t*-BHP in human hepatoma HepG2 cells was investigated in details. We did observe DNA fragmentation as well as typical chromatin condensation and nuclear fragmentation shown by Hoechst staining. Moreover, the apoptotic pathway induced by *t*-BHP involves the activation of caspases. Previous studies have already described induction of apoptosis in HepG2 cells by *t*-BHP [15,16], but this work describes in details for the first time the signaling pathway initiated by *t*-BHP and the kinetics of this pathway and evidenced that mitochondria play a crucial role in the *t*-BHP-induced apoptosis. *t*-BHP was shown to induce cytochrome *c* release from mitochondria isolated from mouse liver [17]. Here, we showed that *t*-BHP was able to induce cytochrome *c* release from mitochondria in whole cells. In addition, the involvement of MPTP in the apoptotic process induced by *t*-BHP was suggested by the fact that two inhibitors of MPTP, CyA and BA, decreased the DNA

fragmentation induced by *t*-BHP. Moreover, *t*-BHP-induced a depolarization of the mitochondrial membrane potential preceded by hyperpolarization. *t*-BHP has also been described to induce mitochondrial permeability transition in hepatocytes [6,7]. In *t*-BHP-treated hepatocytes, NAD(P)H oxidation and ROS formation are critical events promoting MPTP [7]. In these cells, *t*-BHP is metabolized by the glutathione peroxidase-glutathione reductase system, leading to oxidation of glutathione and reduced pyridine nucleotides (NAD(P)H) [7]. Costantini *et al.* [18] showed that the opening of MPTP depends on two distinct sites in the pore (the P and the S sites) which are sensitive to the oxidation-reduction state of pyridine nucleotides (PN) and of glutathione, respectively. As *t*-BHP can oxidize both PN and glutathione, it can affect MPTP by acting at both P and S sites. Moreover, Petronilli *et al.* [19] showed that the opening of MPTP depends on the oxidation-reduction state of vicinal thiols in cysteinyl residues present in the S site of MPTP. One of the possible ways by which *t*-BHP-induced MPTP opening in hepato-



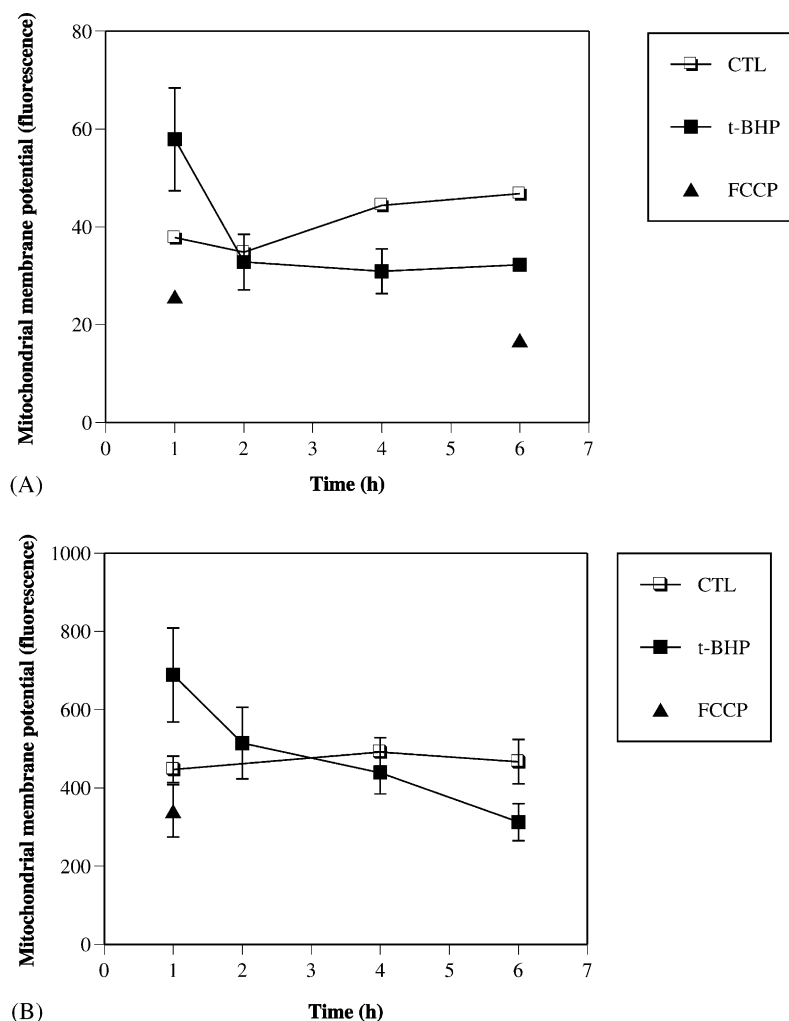


Fig. 6. Mitochondrial membrane potential measurement. (A) Cells seeded on cover slides were incubated with *t*-BHP ( $5 \times 10^{-4}$  M) during increasing time. The TMRE probe was added during the last hour and mitochondrial membrane potential was monitored by following TMRE-associated fluorescence. The uncoupler FCCP (10  $\mu$ M) was added in the medium at the indicated time during the last 15 min. Results are expressed as means  $\pm$  1 SD ( $N = 3$ ) or as means ( $N = 2$ ). (B) Cells seeded on cover slides were incubated with *t*-BHP ( $5 \times 10^{-4}$  M) during increasing time. The rhodamine 123 probe was added during the last 30 min and mitochondrial membrane potential was monitored by following rhodamine 123-associated fluorescence. The uncoupler FCCP (10  $\mu$ M) was added in the medium at the indicated time during the last 35 min. Results are expressed as means  $\pm$  1 SD ( $N = 4$ ).

cytes may be caused by ROS-mediated oxidation of dithiols present in the S site of MPTP [7]. To our knowledge, nothing is known about the action of *t*-BHP on the MPTP opening in hepatoma cells. As the metabolism of *t*-BHP and its action is relatively well documented in hepatocytes, we might assume that *t*-BHP acts in hepatoma cells as it does in hepatocytes. Indeed, we evidenced an induction of ROS production in HepG2 after 1 hr incubation in the presence of *t*-BHP as measured using the fluorescent probe H2DCFDA (data not shown).

It is now well established that caspase activation is the initiating trigger of the apoptosis pathway. The impact that outer mitochondrial membrane permeabilization has on this pathway is less clear. Loss of the mitochondrial membrane potential seems not to be necessary for cytochrome *c* release and caspase activation [20,21]. This is confirmed by our results since caspase activation was observed before (at 1.5 hr for caspase 9 and 2 hr for

caspase 3) loss of the mitochondrial membrane potential (observed at 4 hr incubation). However, the fact that inhibitors of MPTP could inhibit caspase activation and DNA fragmentation suggests that this pore may play a role in the initiating events. Since hyperpolarization was observed very early (at 1 hr incubation), it is possible that it is the hyperpolarization rather than loss of potential which is involved in the release of proteins from the mitochondrial intermembrane space. The kinetics of the apoptotic events initiated in HepG2 cells by *t*-BHP is summarized in Fig. 7. Such a role for hyperpolarization is also suggested by the work of Piacentini *et al.* [22] which shows that transglutaminase overexpression sensitizes neuronal cell lines to apoptosis by increasing mitochondrial membrane potential. Further work will confirm whether this phenomenon is specific to some pro-apoptotic situations or is broadly involved in many programmed cell death events.

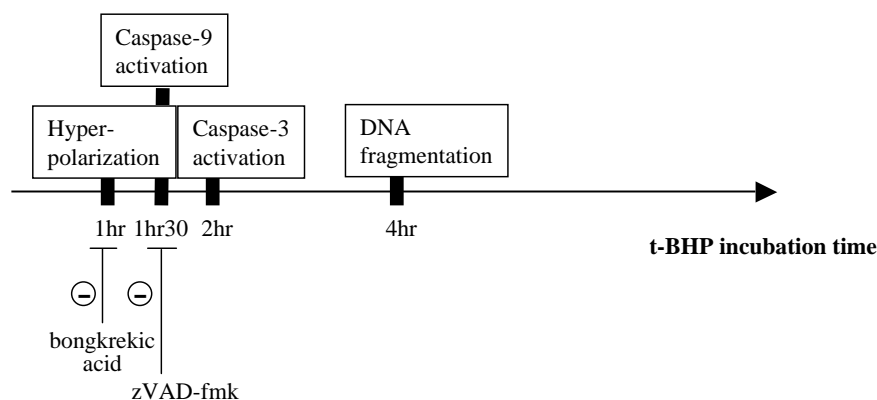


Fig. 7. Schematic representation of the *t*-BHP-induced apoptotic events in HepG2 cells.

## Acknowledgments

J.-P. Piret is a fellow of FRIA (Fonds pour la Recherche dans l'Industrie et l'Agriculture, Belgium). C. Michiels and T. Arnould are Research Associates of FNRS (Fonds National de la Recherche Scientifique, Belgium).

## References

- [1] Vaux DL, Korsmeyer SJ. Cell death in development. *Cell* 1999; 96:245–54.
- [2] Meier P, Finch A, Evan G. Apoptosis in development. *Nature* 2000; 407:796–801.
- [3] Mc Carthy NJ, Smith CA, Williams GT. Apoptosis in the development of the immune system: growth factors clonal selection and Bcl-2. *Cancer Metastasis Rev* 1992;11:157–78.
- [4] Sanchez A, Alvarez AM, Benito M, Fabregat I. Apoptosis induced by transforming growth factor-beta in fetal hepatocyte primary cultures: involvement of reactive oxygen intermediates. *J Biol Chem* 1996;271: 7416–22.
- [5] Kim CH, Yasumoto K, Suzuki T, Yoshida M. *Tert*-butyl hydroperoxide-induced hemolysis of alpha-tocopherol-depleted erythrocytes from selenium-deficient and selenium-adequate rats. *J Nutr Sci Vitaminol* 1988;34:481–90.
- [6] Nieminen AL, Saylor AK, Tesfai SA, Herman B, Lemasters JJ. Contribution of the mitochondrial permeability transition to lethal injury after exposure of hepatocytes to *t*-butylhydroperoxide. *Biochem J* 1995;307:99–106.
- [7] Nieminen AL, Byrne AM, Herman B, Lemasters JJ. Mitochondrial permeability transition in hepatocytes induced by *t*-BuOOH: NAD(P)H and reactive oxygen species. *Am J Physiol* 1997;272: C1286–94.
- [8] Crompton M. The mitochondrial permeability transition pore and its role in cell death. *Biochem J* 1999;341:233–49.
- [9] Gross A, McDonnell JM, Korsmeyer SJ. BCL-2 family members and the mitochondria in apoptosis. *Genes Dev* 1999;13:1899–911.
- [10] Desagher S, Martinou JC. Mitochondria as the central control point of apoptosis. *Trends Cell Biol* 2000;10:369–77.
- [11] Crompton M, Virji S, Doyle V, Johnson N, Ward JM. The mitochondrial permeability transition pore. *Biochem Soc Symp* 1999;66:167–79.
- [12] Bossy-Wetzel E, Green DR. Apoptosis: checkpoint at the mitochondrial frontier. *Mutat Res* 1999;434:243–51.
- [13] Broekemeier KM, Dempsey ME, Pfeiffer DR. Cyclosporin A is a potent inhibitor of the inner membrane permeability transition in liver mitochondria. *J Biol Chem* 1989;264:7826–30.
- [14] Marchetti P, Castedo M, Susin SA, Zamzami N, Hirsch T, Macho A, Haeflner A, Hirsch F, Geuskens M, Kroemer G. Mitochondrial permeability transition is a central coordinating event of apoptosis. *J Exp Med* 1996;184:1155–60.
- [15] Kim JA, Kang YS, Kim YO, Lee SH, Lee YS. Role of  $\text{Ca}^{2+}$  influx in the *tert*-butyl hydroperoxide-induced apoptosis of HepG2 human hepatoblastoma cells. *Exp Mol Med* 1998;30:137–44.
- [16] Kim JA, Kang YS, Lee SH, Lee YS. Inhibitors of  $\text{Na}^{+}/\text{Ca}^{2+}$  exchanger prevent oxidant-induced intracellular  $\text{Ca}^{2+}$  increase and apoptosis in a human hepatoma cell line. *Free Radic Res* 2000;33:267–77.
- [17] Yang JC, Cortopassi GA. Induction of the mitochondrial permeability transition causes release of the apoptogenic factor cytochrome *c*. *Free Radic Biol Med* 1998;24:624–31.
- [18] Costantini P, Chernyak BV, Petronilli V, Bernardi P. Modulation of the mitochondrial permeability transition pore by pyridine nucleotides and dithiol oxidation at two separate sites. *J Biol Chem* 1996;271:6746–51.
- [19] Petronilli V, Costantini P, Scorrano L, Colonna R, Passamonti S, Bernardi P. The voltage sensor of the mitochondrial permeability transition pore is tuned by the oxidation/reduction state of vicinal thiols. Increase of the gating potential by oxidants and its reversal by reducing agents. *J Biol Chem* 1994;269:16638–42.
- [20] Waterhouse NJ, Goldstein JC, von Ahsen O, Schuler M, Newmeyer DD, Green DR. Cytochrome *c* maintains mitochondrial transmembrane potential and ATP generation after outer mitochondrial membrane permeabilization during the apoptotic process. *J Cell Biol* 2001;153:319–28.
- [21] Waterhouse NJ, Ricci JE, Green DR. And all of a sudden it's over: mitochondrial outer-membrane permeabilization in apoptosis. *Biochimie* 2002;84:113–21.
- [22] Piacentini M, Farrace MG, Piredda L, Matarrese P, Ciccocanti F, Falasca L, Rodolfo C, Giammarioli AM, Verderio E, Griffin M, Malorni W. Transglutaminase overexpression sensitizes neuronal cell lines to apoptosis by increasing mitochondrial membrane potential and cellular oxidative stress. *J Neurochem* 2002;81:1061–72.